Supplemental Information

Epigenetic regulation of transcriptional plasticity is associated with developmental song learning

Theresa K Kelly, Somayeh Ahmadiantehrani, Adam Blattler, Sarah E London

SUPPLEMENTAL FIGURES AND TABLES

Figure S1. Modified screenshot of UCSC Genome Browser showing custom tracks of H3K9me3, H3K27me3, H3K4me3, and Pol2 data for Tutored and Isolate auditory forebrain. Note H3K4me3 and Pol2 are located proximal to the transcriptional start sites (gene models in blue at the bottom); H3K9me3 and H3K27me3 peaks are broader and more distal to gene bodies.

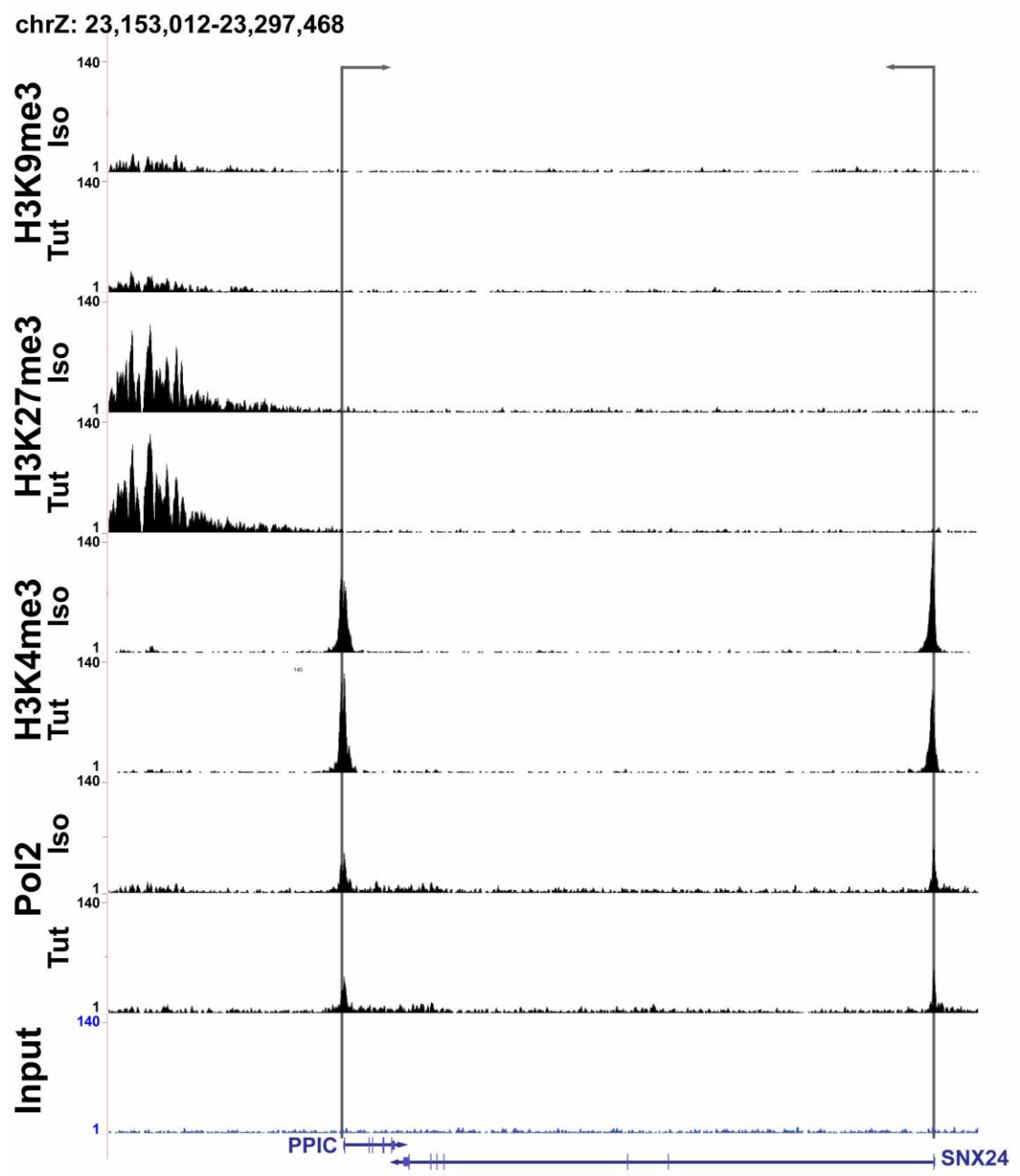

Figure S2. Pearson Correlation Coefficients demonstrate higher correlations of read count density within called peaks between two markers of active chromatin, H3K4me3 and Pol2, and between two markers of repressed chromatin, H3K9me3 and H3K27me3, than across active and repressed data. For example, the correlation between H3K4me3 and Pol2 Isolate data is 0.74, but only 0.297 between H3K4me3 and H3K9me3 Isolate data. I.1 = Isolate, T.1 = Tutored.

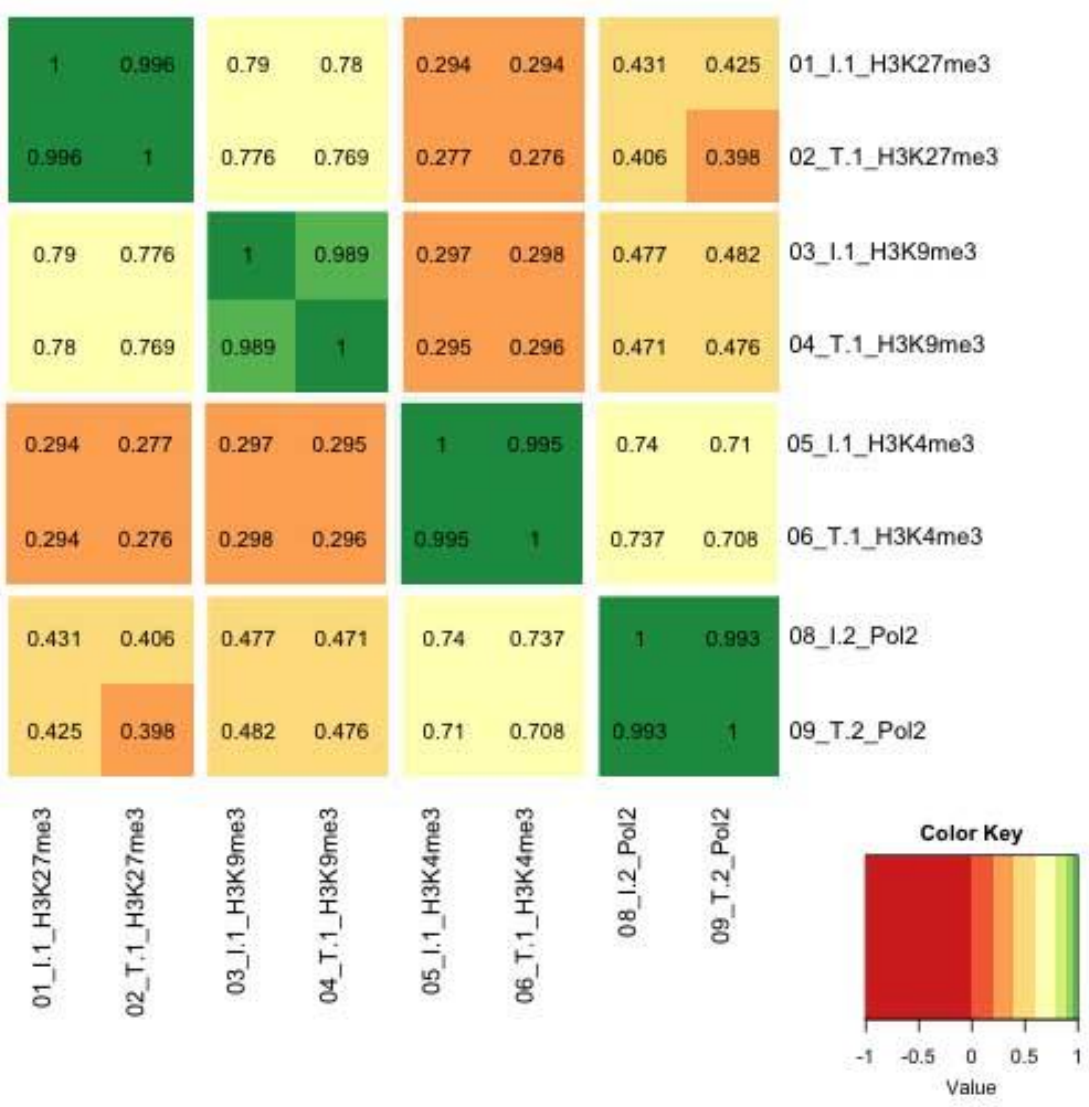

Figure S3. A second replicate of ChIPseq with an independent set of P67 Tutored and Isolate birds confirms central findings. (A) Song similarity scores are higher for Tutored than Isolate birds (t-test p = 0.02). Shown is the highest of the three possible scores for each Isolate. Symbols designate which tutor comparison is depicted, and the numbers on the graphs indicate the quantitative difference in song similarity score between the Tutored-tutor and Isolate-tutor analyses when they are evaluated against the same tutor bird. (B) Scatterplots of the number of reads (x and y axes) per called peak positions (dots) for Replicate 1 and Replicate 2 ChIPseq data. PC = Pearson Correlation Coefficients demonstrating high correspondence between the two datasets. (C) Screenshots of from UCSC Genome Browser illustrating the highly-similar patterns of ChIPseq read distributions between Replicate 1 Tutored (top row), Replicate 1 Isolate (second row down), Replicate 2 Tutored (third row down) and Replicate 2 Isolate (bottom row). Top left = H3K9me3, top right = H3K27me3, bottom left = H3K4me3, bottom right = Pol2. (D) The number of genes that were differentially associated with H3K9me3, H3K27me3, H3K4me3 and Pol2 in Replicate 2 verify the finding that more genes are associated with H3K9me3 and H3K27me3 modifications in the Tutored compared to the Isolate auditory forebrain, and that more genes are associated with H3K4me3 and Pol2 in the Isolate compared to the Tutored auditory forebrain. The number of Isolate and Tutored genes differentially associated with H3K9me3 (Tutored: 691, Isolate: 322), H3K27me3 (Tutored: 413, Isolate: 314), H3K4me3 (Tutored: 391, Isolate: 1374), and Pol2 (Tutored: 212, Isolate: 2422) in Replicate 2. * designates significantly different proportions at $p < 0.01$.

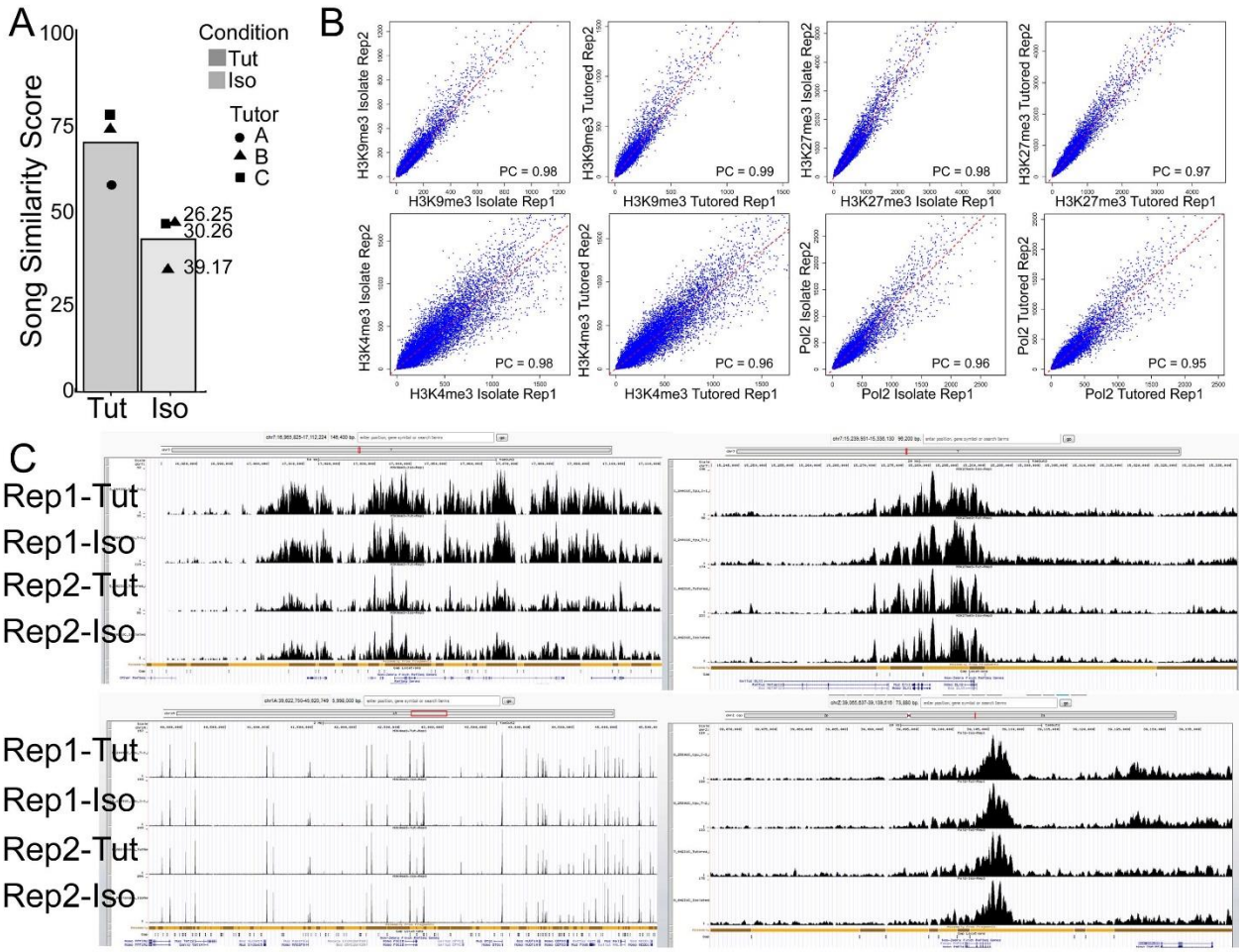
A
Song Similarity Score
100
75
50
25
0
Tut
Iso
Condition
Tut
Iso
Tutor
A
B
C
26.25
30.26
39.17
B
H3K9me3 Isolate Rep2
H3K9me3 Isolate Rep1
PC = 0.98
H3K9me3 Tutored Rep2
H3K9me3 Tutored Rep1
PC = 0.99
H3K27me3 Isolate Rep2
H3K27me3 Isolate Rep1
PC = 0.98
H3K27me3 Tutored Rep2
H3K27me3 Tutored Rep1
PC = 0.97
H3K4me3 Isolate Rep2
H3K4me3 Isolate Rep1
PC = 0.98
H3K4me3 Tutored Rep2
H3K4me3 Tutored Rep1
PC = 0.96
Pol2 Isolate Rep2
Pol2 Isolate Rep1
PC = 0.96
Pol2 Tutored Rep2
Pol2 Tutored Rep1
PC = 0.95
C
Rep1-Tut
Rep1-Iso
Rep2-Tut
Rep2-Iso
Rep1-Tut
Rep1-Iso
Rep2-Tut
Rep2-Iso
D
Differential Genes
2500
2000
1500
1000
500
0
Tutored
Isolate
*
*
*
*
H3K9me3
H3K27me3
H3K4me3
Pol2

Table S1. Biological ChIPseq replicate GO categories at Fisher's test of adjusted p-values ($\alpha < 0.05$).

Significantly underrepresented are designated with *.

GO ID	GO description	Expected	Observed	Adj. Fisher
Isolate-on				
GO:0005634	nucleus	1017	1247	7.60E-23
GO:0004930	G-protein coupled receptor activity	192	95	9.90E-20 *
GO:0007186	G-protein coupled receptor signaling pathway	250	142	8.60E-19 *
GO:0005739	mitochondrion	361	482	1.20E-15
GO:0004871	signal transducer activity	236	143	2.10E-14 *
GO:0004872	receptor activity	268	170	3.70E-14 *
GO:0005737	cytoplasm	833	992	9.80E-13
GO:0003677	DNA binding	408	514	2.70E-10
GO:0005515	protein binding	2499	2703	2.70E-10
GO:0016021	integral to membrane	816	682	4.40E-09 *
GO:0007165	signal transduction	422	324	7.30E-09 *
GO:0006334	nucleosome assembly	30	55	2.80E-07
GO:0000786	nucleosome	27	49	1.30E-06
GO:0045944	positive regulation of transcription from RNA polymerase II promoter	177	231	1.80E-05
GO:0005694	chromosome	37	61	3.10E-05
GO:0005200	structural constituent of cytoskeleton	52	26	0.00025 *
GO:0043565	sequence-specific DNA binding	194	244	0.00027
GO:0003676	nucleic acid binding	432	360	0.00033 *
GO:0008270	zinc ion binding	626	545	0.001 *
GO:0003964	RNA-directed DNA polymerase activity	14	2	0.0022 *
GO:0006278	RNA-dependent DNA replication	14	2	0.0022 *
GO:0006355	regulation of transcription, DNA-dependent	302	357	0.003
GO:0005882	intermediate filament	64	38	0.003 *
GO:0005813	centrosome	77	104	0.009
GO:0008284	positive regulation of cell proliferation	78	104	0.019
GO:0003700	sequence-specific DNA binding transcription factor activity	233	277	0.02
GO:0045892	negative regulation of transcription, DNA-dependent	100	128	0.028
GO:0006139	nucleobase-containing compound metabolic process	19	32	0.032
GO:0005730	nucleolus	111	140	0.035
GO:0005874	microtubule	39	56	0.038
GO:0010212	response to ionizing radiation	9	18	0.038
GO:0006352	transcription initiation, DNA-dependent	9	18	0.038
GO:0022625	cytosolic large ribosomal subunit	15	26	0.041
GO:0005829	cytosol	125	155	0.042
Tutored-on				
GO:0000786	nucleosome	5	31	3.60E-16
GO:0006334	nucleosome assembly	5	31	2.10E-14
GO:0005694	chromosome	6	33	2.20E-13
GO:0045653	negative regulation of megakaryocyte differentiation	0	6	0.00012

Table S2. Gene Ontology Molecular Function and Biological Process categories, as well as Panther Protein Classes, represented in all datasets show overlap between datasets that predict greater transcription in Tutored-on and Isolate-on gene sets. “y” indicates that a particular dataset is represented for the functional category in each row.

	Tutored-on				Isolate-on			
	H3K9me3 - Iso	H3K27me3 - Iso	H3K4me3 - Tut	Pol2 - Tut	H3K9me3 -TuT	H3K27me3 - Tut	H3K4me3 - Iso	Pol2 - Iso
molecular function								
binding (GO:0005488)	y	y	y	y	y	y	y	y
catalytic activity (GO:0003824)	y	y	y	y	y	y	y	y
enzyme regulator activity (GO:0030234)	y	y	y	y	y	y	y	y
nucleic acid binding transcription factor activity (GO:0001071)	y	y	y	y	y	y	y	y
receptor activity (GO:0004872)	y	y	y	y	y	y	y	y
structural molecule activity (GO:0005198)	y	y	y	y	y	y	y	y
translation regulator activity (GO:0045182)			y		y	y	y	y
transporter activity (GO:0005215)	y	y	y	y	y	y	y	y
channel regulator activity (GO:0016247)						y		y
protein binding transcription factor activity (GO:0000988)		y	y	y		y	y	y
antioxidant activity (GO:0016209)							y	y
biological process								
apoptotic process (GO:0006915)	y	y	y	y	y	y	y	y
biological adhesion (GO:0022610)	y	y	y	y	y	y	y	y
biological regulation (GO:0065007)	y	y	y	y	y	y	y	y
cellular component organization or biogenesis (GO:0071840)	y	y	y	y	y	y	y	y
cellular process (GO:0009987)	y	y	y	y	y	y	y	y
developmental process (GO:0032502)	y	y	y	y	y	y	y	y
immune system process (GO:0002376)	y	y	y	y	y	y	y	y
localization (GO:0051179)	y	y	y	y	y	y	y	y
locomotion (GO:0040011)			y	y		y	y	y
metabolic process (GO:0008152)	y	y	y	y	y	y	y	y
multicellular organismal process (GO:0032501)	y	y	y	y	y	y	y	y
reproduction (GO:0000003)	y	y	y	y		y	y	y
response to stimulus (GO:0050896)	y	y	y	y	y	y	y	y
protein class								
calcium-binding protein (PC00060)		y	y	y	y	y	y	y
cell adhesion molecule (PC00069)	y	y	y	y	y	y	y	y
cell junction protein (PC00070)		y	y	y	y	y	y	y
chaperone (PC00072)			y			y	y	y
cytoskeletal protein (PC00085)	y	y	y	y	y	y	y	y
defense/immunity protein (PC00090)	y	y	y	y	y	y	y	y
enzyme modulator (PC00095)	y	y	y	y	y	y	y	y
extracellular matrix protein (PC00102)	y	y	y	y	y	y	y	y
hydrolase (PC00121)	y	y	y	y	y	y	y	y
isomerase (PC00135)			y	y	y	y	y	y
kinase (PC00137)		y	y	y	y	y	y	y
ligase (PC00142)			y	y	y	y	y	y
lyase (PC00144)			y			y	y	y

membrane traffic protein (PC00150)	y	y	y	y	y	y	y	y
nucleic acid binding (PC00171)	y	y	y	y	y	y	y	y
oxidoreductase (PC00176)	y	y	y	y	y	y	y	y
phosphatase (PC00181)	y	y	y	y	y	y	y	y
protease (PC00190)	y	y	y	y	y	y	y	y
receptor (PC00197)	y	y	y	y	y	y	y	y
signaling molecule (PC00207)	y	y	y	y	y	y	y	y
storage protein (PC00210)						y	y	
structural protein (PC00211)				y		y	y	y
surfactant (PC00212)	y		y	y	y	y	y	y
transcription factor (PC00218)	y	y	y	y	y	y	y	y
transfer/carrier protein (PC00219)	y	y	y	y	y	y	y	y
transferase (PC00220)		y	y	y	y	y	y	y
transmembrane receptor regulatory/adaptor protein (PC00226)	y	y	y	y		y	y	y
transporter (PC00227)	y	y	y	y	y	y	y	y

Figure S4. High individual gene specificity represents similar biological processes - but in opposite directions - across Tutored and Isolate datasets. Ingenuity Pathway Analysis of biological processes showed a large overlap in the functional processes represented in ChIPseq genesets, as indicated by numbers indicating the same process in Tutored-on (left panel, top) and Isolate-on (left panel, bottom), but with predicted gene expression patterns in opposite directions (orange is upregulated, blue is downregulated; color intensity indicates magnitude of difference). An example of the array of genes contained within one of these differential processes, Development of Neurons, is circled in the left panels and displayed in more detail in the right panels. Right panels illustrate that nearly all genes are either relatively up- (red symbols) or down-regulated (green symbols) in Isolate and Tutored samples, respectively. Gray diagonal lines simply visually connect the gene nodes with the main function, development of neurons. Categories identified in left panel are: 1 : organismal development, 2 : tissue development, 3 : gastrointestinal disease, 4 : embryonic development, 5 : skeletal and muscular system development, 6 : cellular growth and proliferation, 7 : organ development, 8 : tissue, morphology, 9 : cellular development, 10 : nervous system development, 11 : cardiovascular development, 12 : cellular movement, 13 : developmental disorder, 14 : connective tissue development, 15 : cellular function, 16 : gene expression, 17 : cellular assembly and organization, 18 : cardiovascular disease, 19 : respiratory disease, 20 : organ morphology.

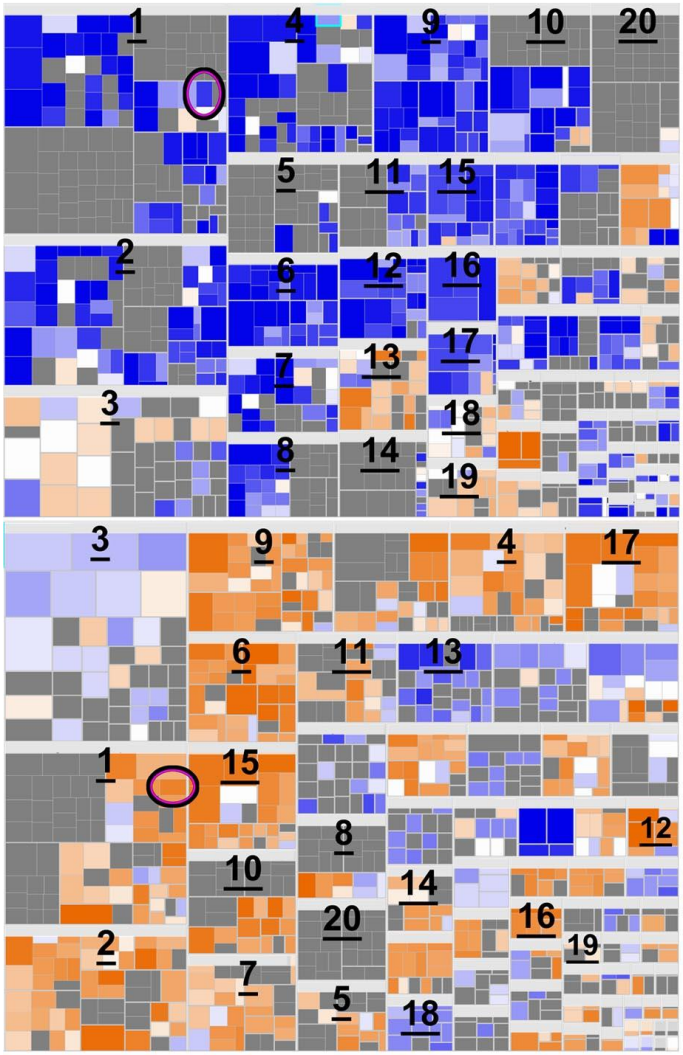
1
4
9
10
20
5
11
15
2
6
12
16
17
7
13
3
18
8
14
19
3
9
4
17
6
11
13
1
15
8
12
10
14
20
16
19
2
7
5
18

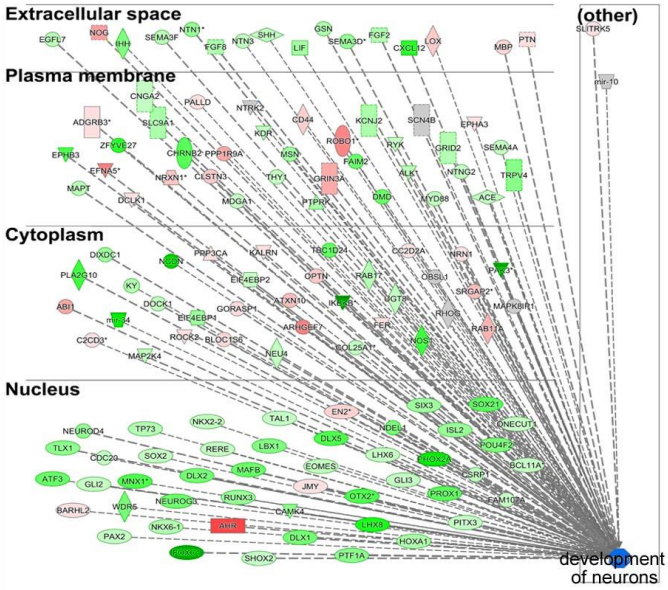
Extracellular space
Plasma membrane
Cytoplasm
Nucleus
(other)
development of neurons

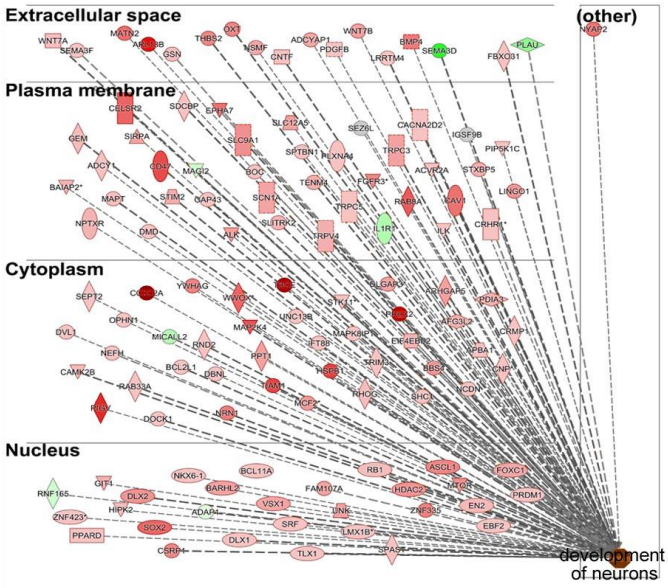
Extracellular space
Plasma membrane
Cytoplasm
Nucleus
(other)
development of neurons

Table S3. List of genes that comprise the Development of Neurons category in IPA analysis.

Tutored				Isolate		
SOX21	PAX2	CDLK1	LIF	FOXC1	PPT1	SLC9A1
ONECUT	FOXC1	ADGRB3	GSN	PRDM1	TIAM1	BOC
SIX3	SHOX1	ZFYVE27	SEMA3D	ASCL1	MCF2	SCN1A
ISL2	PTF1A	NRXN1	FGF2	MTOR	CC2C2A	SLITRK2
POU4F2	MAP2K4	CNGA2	CXCL12	EN2	MAP2K4	TRPV4
BCL11A	C2CD3	SLC9A1	LOX	EBF2	HSPB1	SLC12A5
EN2	ABI1	CHRNB2	MBP	RB1	RHOG	SPTBN1
NDEL1	mir-34	SLSTN3	PTN	HDAC2	YWHAG	TENM4
PHOX2A	PLA2G10	MDGA1		ZNF335	WWOX	TRPC5
CSRP1	DIXDC1	PALLD		BCL11A	UNC13B	IL1R1
FAM107A	ROCK2	PPP1R9A		FAM107A	IFT88	PLXNA4
TAL1	BLOC1S6	THY1		NKX6-1	TBCE	FGFR3
DLX5	NEU4	PTPRK		BARHL2	MAPK8IP1	SEZ6L
LHX6	EIF4EBP4	NTRK2		VSX1	TRIM3	TRPC3
NKX2-2	DOCK1	KDR		UNK	SHC1	RAB8A
LBX1	KY	MSN		GIT1	STK11	CACNA2D2
EOMES	NCDN	GRIN3A		DLX2	EIF4EBP2	ACVR2A
GLI3	GORASP1	CD44		ADAP1	BBS4	CAV1
POX1	PRP3CA	ROBO1		SRF	NCDN	IGSF9B
TP73	EIFEBP2	FAIM2		LMX1B	DLGAP3	STXBP5
RERE	ATXN10	DMD		RNF165	PREX2	CRHR1
NEUROD4	ARGHEF7	KCNJ2		HIPK2	ARHGAP5	PIP5K1C
MAFB	COL25A1	RYK		ZNF423	AFG3L2	LINGO1
JMY	KALRN	ALK		PPARD	APBA1	WNT7A
OTX2	OPTN	MYD88		SOX2	CNP	SEMA3F
PITX3	IKBKB	SCN4B		CSRP1	PDIA3	MATN2
TLX1	FER	GRID2		DLX1	CRMP1	ARL13B
CDC20	NOS1	NTNG2		TLX1	NPTXR	GSN
DLX2	TBC1D24	ACE		SPAST	BAIAP2	THBS2
MNX1	RAB17	EPHA3		PIGV	MAPT	OXT
RUNX3	UGT8	SEMA4A		DOCK1	DMD	NSMF
ATF3	CC2D2A	TRPV4		CAMK2B	GEM	CNTF
GLI2	OBSL1	mir-10		RAB33A	ADCY1	ADCYAP1
NEUROG3	RHOG	SLITRK5		NRN1	CELSR2	PDGFB
CAMK4	NRN1	EGFL7		DVL1	SIRPA	WNT7B
LHX8	SRGAR2	NOG		NEFH	CD47	LRRTM4
WDR5	RAB11A	IHH		BCL2L1	STIM2	BMP4
BARHL2	PAK3	SEMA3F		DBNL	GAP43	SEMA3D
NKX6-1	MAPK8IP1	NTN1		OPHN1	ALK	FBXO31
AHR	MAPT	FGF8		SEPT2	MAGI2	PLAU
DLX1	EPHB3	NTN3		MICALL2	SDCBP	NYAP2
HOXA1	EFNA5	SHH		RND2	EPHA7	

Table S5. 350 genes of the Isolate-on overrepresented GO categories associated with transcription.

Symbol	Symbol	Symbol	Symbol	Symbol	Symbol	Symbol	Symbol
SCAMP1	TNIK	H3F3B	PTPRS	TSHZ1	FAM107A	FAT2	GLRB
SOX3	EBF2	RPL11	CLDN4	POU2F3	ZBTB8A	RORB	ARR3
RAP1A	THBS2	CDK10	CREBRF	PKM	TLX1	NTM	JMJD6
REEP5	DDX41	PCGF5	SRSF6	KIF21A	MSX1	ATR	ARIH2
BNIP1	FAF2	ACAT2	ANKRD44	BARHL2	YWHAQ	CHD1L	RBBP4
NUP35	FGF1	PCBD2	DNAJB5	IMP3	PKP1	TRPC5	WDR73
HMGN5	CDC23	SDCBP2	PHF5A	COMMD5	PHC1	NAA50	KDM2A
RPF2	USP7	PTK7	VPS11	CC2D2A	AFG3L2	GAP43	ZBTB25
ISCU	EIF4EBP2	BCL2L1	POLE3	FGFR3	SDCBP	GIT2	DLX6
ATP5F1	ANKRD66	CTNNBL1	PODN	MTF1	SNX33	WASF2	SYT2
ANKRD49	RAB33A	TRAIP	TWIST1	SF3B3	INTS1	PSMB2	GLYCTK
NFU1	TDRD7	PRKDC	FHL1	CCNG1	TCEANC2	LIN28A	WIPI1
YWHAG	STK16	BAP1	CADPS	EXOC8	DNAI1	P4HA2	ZNF319
HMOX2	MID2	FUBP1	OPHN1	SLC9A3R2	SIN3B	BET1L	CIAPIN1
CIRBP	MYO1D	SPARC	CORO1C	TBL3	CDC34	CD47	ACVR2B
PRELID1	RRAGA	NKX2-5	ADPRHL2	CD72	SUN2	MOB2	WDR18
MDH2	EXOSC1	PLCL1	MYCL	PIAS4	FAT3	KCNA2	TBXA2R
EDF1	TRIM63	PCDH18	CRMP1	SRR	ST14	ZIC1	RXRA
PPIC	KLHDC4	HSPB1	GATA6	PIGO	MYD88	PLEKHO1	GTF3C6
SAT1	VAC14	HMG20B	AP3M2	RFX2	MCM3	KLHL17	C4
LSM4	WTAP	SMTNL2	LRRTM4	WNT8A	EXOC7	NKX6-3	GRIK2
MED6	DDB1	SEMA3D	SAMD13	ETS1	CDC27	RAX2	DVL1
DRD2	HM13	VANGL1	GAN	TRIL	NIPA2	DARS	ELOVL6
ADARB2	ANAPC1	SETD1B	SIGMAR1	MTOR	NSUN2	SGCD	RRP8
TLN1	CBX4	YARS	AP2B1	CAMK1	MAPK8IP1	HIPK2	RSPO1
APBA3	SCNN1A	RUNX3	SERPINE2	GJB3	SPOCK1	CBL	RPL13
APBA1	FKBP5	MC1R	SOCS2	CUTC	SNX21	FOPNL	NUP160
ADAM23	TTC4	MMS19	NETO1	XPO1	IKZF2	VAMP3	CCND1
SH2D3C	STXBP5	STK4	GRHL3	KDM5B	NDUFB10	ABCC1	
IL10RA	PPP1R3C	FOXI1	RIC8A	MYSM1	BCOR	EZH1	EPHA1
PER3	ZNF462	SIRT3	RPS6KC1	GINS4	MMP15	IGBP1	SIN3A
AP1G1	NR2C2	H3F3A	KCNJ2	CNN2	MAP3K5	SRSF2	NMRK2
ORAI1	DHX57	GNAI2	TSR1	WNT7A	PRPF8	PTPRU	TRAPPC3
MYOM3	ANXA6	BTBD17	CSTF3	TP73	RNF44	ARRB1	TGFB3
POLE2	WT1	ADIPOR1	CHAF1A	SPOCK2	UNC13B	SPTB	GID8
ZBTB1	SHH	PAK6	RNF145	BRPF1	EPHA7	PRDM6	NEURL2
ONECUT3	EIF3A	PITX1	WDFY1	EDA	ILKAP	GINS3	CHD4
RAB8A	FOXL2	FGF2	LRRC3	IMPDH2	ZPR1	ELAVL1	SH3BP4
GLA	RGS10	PRPF6	RNF219	SFN	DERL1	MIS12	DAPK3
WHRN	HSPH1	SAMD4A	UBN2	NCDN	ERI3	CORO6	CSF
HDAC2	SPAST	MRPL51	XRN1	RPN2	MAFK	TOR2A	COASY
ACTR5	CRHBP	CSRP1	MTTP	OSBPL10	EIF2B3	CRYAB	ASPSCR1
KLHDC1	ARIH1	SHMT1	UBIAD1	EVX1	COMMD4	TRIP4	SOX7
SRPX2	DLX1	LINGO1	ING1	MYO9A	CNTFR	MYH11	

Figure S5. Descriptive plots of RNAseq analysis. Top is the MA plot of the log2 fold-change (log2FC) between Tutored and Isolate samples plotted according to the mean normalized read count per transcript. Red dots are transcripts with p<0.1. Bottom graphs represent the read counts for individual Tutored and Isolate samples for a subset of transcripts; circles are individual data points and lines represent group means.

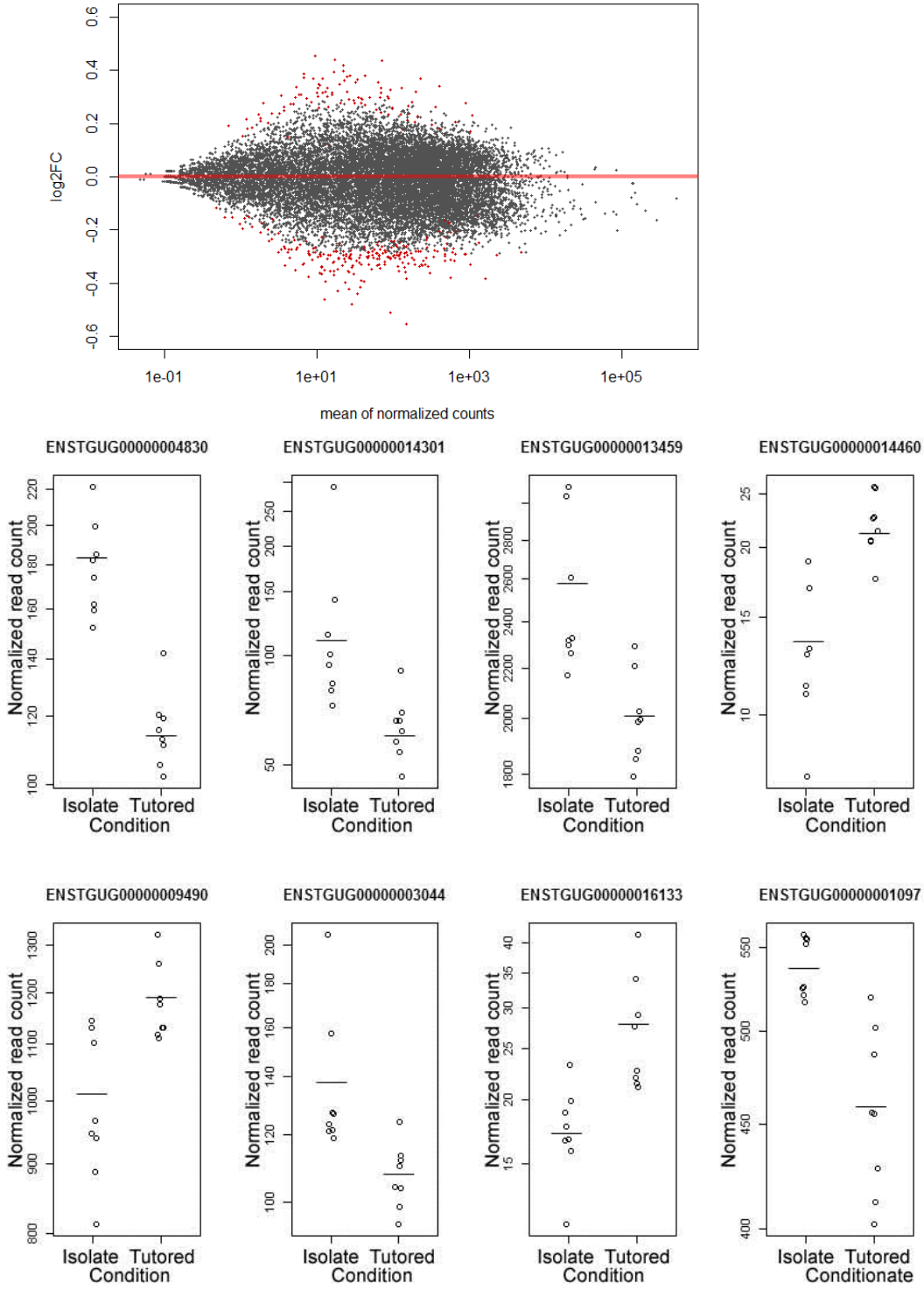

Table S6. RNAseq GO categories. The lowest adjusted p-value for RNAs more abundant in Isolate compared to Tutored (RNAseq_Isolate) and those more abundant in Tutored (RNAseq_Tutored) was 0.11. We therefore report these categories as non-statistically significant insight into functional categories, as we note that genomic and transcriptional regulation is represented in the RNAseq_Isolate but not the RNAseq_Tutored transcriptional profiles.

GO	go_description	expectation	observation	Adj.fisher
RNAseq_Isolate				
GO:0006268	DNA unwinding involved in replication	0	2	0.11
GO:0003678	DNA helicase activity	0	2	0.11
GO:0032508	DNA duplex unwinding	0	2	0.11
GO:0010629	negative regulation of gene expression	0	3	0.11
GO:0035267	NuA4 histone acetyltransferase complex	0	2	0.11
GO:0003697	single-stranded DNA binding	0	2	0.11
GO:0006888	ER to Golgi vesicle-mediated transport	0	2	0.11
GO:0031668	cellular response to extracellular stimulus	0	2	0.11
GO:0032481	positive regulation of type I interferon production	0	2	0.11
GO:0050680	negative regulation of epithelial cell proliferation	0	3	0.11
GO:0005576	extracellular region	4	10	0.11
GO:0050679	positive regulation of epithelial cell proliferation	0	3	0.11
GO:0045600	positive regulation of fat cell differentiation	0	2	0.11
GO:0040014	regulation of multicellular organism growth	0	2	0.11
GO:0007165	signal transduction	11	3	0.11
GO:0045785	positive regulation of cell adhesion	0	2	0.11
GO:0008219	cell death	0	2	0.11
GO:0004129	cytochrome-c oxidase activity	0	2	0.11
GO:0005179	hormone activity	1	3	0.11
GO:0004872	receptor activity	7	1	0.11
GO:0006807	nitrogen compound metabolic process	0	2	0.11
GO:0015630	microtubule cytoskeleton	1	3	0.11
GO:0046332	SMAD binding	0	2	0.11
GO	**go_description**	**expectation**	**observation**	**Adj.fisher**
RNAseq_Tutored				
GO:0019205	nucleobase-containing compound kinase activity	0	2	0.1
GO:0015293	symporter activity	0	2	0.1
GO:0005328	neurotransmitter:sodium symporter activity	0	2	0.1
GO:0006836	neurotransmitter transport	0	2	0.1
GO:0016758	transferase activity, transferring hexosyl groups	0	2	0.11

Table S7. Thirty-nine microRNA genes were differentially associated with PTM and Pol2 (list from ChIPseq Rep1).

	microRNA
H3K27me3 Tutored	MIR10A
	MIR126
	MIR133-2
	MIR15C
	MIR16C
	MIR218-2
	MIR2188
	MIR2956-1
	MIR2956-2
	MIR2976-3
	MIR2994
	MIR34A
	MIR375
	MIR460A
H3K27me3 Isolate	MIR2960
H3K4me3 Tutored	MIR2969
H3K4me3 Isolate	MIR135B
	MIR146B
	MIR15C
	MIR16C
	MIR223

	microRNA
Pol2 Tutored	MIR128-2
	MIR25
	MIR551
Pol2 Isolate	MIR135B
	MIR137
	MIR139
	MIR144
	MIR17A
	MIR18A
	MIR19A
	MIR19B-1
	MIR20A
	MIR2970
	MIR2976-3
	MIR425
	MIR451
	MIR9-1
	MIR92-1

Table S8. Position weight matrices based on genesets predictive of higher transcription in Isolate or Tutored auditory forebrain. Listed are transcription factor binding sites from Transfac and Jaspar databases that were unique for Isolate and Tutored genes (list from ChIPseq Rep1).

Transcription factor	TFBS
Isolate	
AR	V_AR_02
	V_AR_03
	V_AR_Q2
	V_AR_Q6
ATF1	V_ATF_B
ATF1, ATF2, ATF3*, ATF4, ATF5, ATF6, ATF7, CREB1, CREM	V_CREBATF_Q6
ATF1, ATF2, ATF3*, ATF4, ATF7, CREB1, CREM	V_CREB_Q3
ATF2	V_CREBP1_Q2
ATF2, JUN	V_CREBP1CJUN_01
BACH2	V_BACH2_01
CEBPA	V_CEBP_C
	V_CEBP_Q2
CEBPA, CEBPB, CEBPD, CEBPE, CEBPG	V_CEBP_Q2_01
CEBPB*	V_CEBPB_01
CEBPG	V_CEBPGAMMA_Q6
CREB1	V_CREB_01
	V_CREB_Q2
	V_CREB_Q4
CREB1, CREM	V_CREB_Q2_01
	V_CREB_Q4_01
CREB1, CREM, ATF1, ATF2, ATF3, ATF4, ATF7	V_CREB_Q3
CREB1, CREM, ATF1, ATF2, ATF3, ATF4, ATF5, ATF6, ATF7	V_CREBATF_Q6
EGR3	V_EGR3_01
FOS, FOSB, FOSL1, FOSL2, JUN, JUND	V_AP1_C
	V_AP1_Q2
	V_AP1_Q4
	V_AP1_Q6
	V_AP1FJ_Q2
FOS, FOSB, FOSL1, FOSL2, JUN, JUNB, JUND	V_AP1_01
	V_AP1_Q2_01
	V_AP1_Q4_01
	V_AP1_Q6_01
GATA2*	V_GATA2_01
	V_GATA2_02
	V_GATA2_03
HLF	V_HLF_01
HOXA9, MEIS1	V_MEIS1AHOXA9_01
	V_MEIS1BHOXA9_02
HP1	V_HP1SITEFACTOR
IRF1, IRF2, IRF3, IRF4*, IRF5, IRF6, IRF7, IRF8	V_IRF_Q6
IRF1, IRF2, IRF3, IRF4*, IRF5, IRF7, IRF8, IRF9	V_IRF_Q6_01
MAF	V_MAF_Q6
MEF2A*	V_AMEF2_Q6

* TF also in Isolate-on dataset

‡ TF also in Tutored-on dataset

	V_MEF2_01
	V_MEF2_04
	V_MMEF2_Q6
MEIS1	V_MEIS1_01
NFATC1, NFATC2‡, NFATC3, NFATC4	V_NFAT_Q4_01
	V_NFAT_Q6
NFE2L1	V_TCF11_01
NFIA, NFIC	V_NF1_Q6_01
NFKB1, NFKB2	V_NFKB_C
NFKB1, RELA	V_NFKAPPAB_01
NFYA, NFYB, NFYC	V_NFY_01
	V_NFY_Q6
	V_NFY_Q6_01
NKX6-2	V_NKX62_Q2
NR1H2-RXR	NR1H2-RXR
NR3C1	NR3C1
PBX1	V_PBX1_01
	V_PBX1_02
	V_PBX1_03
PPARG*	V_PPARG_01
	V_PPARG_02
RELA	V_NFKAPPAB65_01
SOX9*	V_SOX9_B1
SRF*	V_SRF_C
	V_SRF_Q4
	V_SRF_Q6
STAT1	V_STAT1_03
vJUN	V_VJUN_01
XBP1	V_XBP1_01
Tutored	
ESR1‡, ESR2	V_ER_Q6_02
FOXO1	V_FOXO1_01
GATA2	V_GATA2_02
NFATC1, NFATC2‡, NFATC3, NFATC4	V_NFAT_Q4_01
NFKB1	V_NFKAPPAB50_01
NFKB1, NFKB2, RELA	V_NFKB_Q6_01
SRF	V_SRF_01
	V_SRF_C

Figure S6. Cross-referencing Tutored and Isolate genesets with a database of RNAs enriched in distinct cell types (https://web.stanford.edu/group/barres_lab/brain_rnaseq.html) revealed that few, < 5%, of our genes were cell-type specific. Percent of each geneset is mapped below. The ratios of cell-type specific gene number compared to the Isolate-up and Tutored-up genesets (from ChIPseq Rep1) are: Neuron Isolate-up: 30/3181, Tutored-up: 6/628; Astrocyte Isolate-up: 86/3181, Tutored-up: 29/628; Myelinated oligodendrocyte (myelin.oligo) Isolate-up: 89/3181, Tutored-up: 11/628; microglia Isolate-up: 60/3181, Tutored-up: 7/628; endothelial cells Isolate-up: 116/3181, Tutored-up: 12/628.

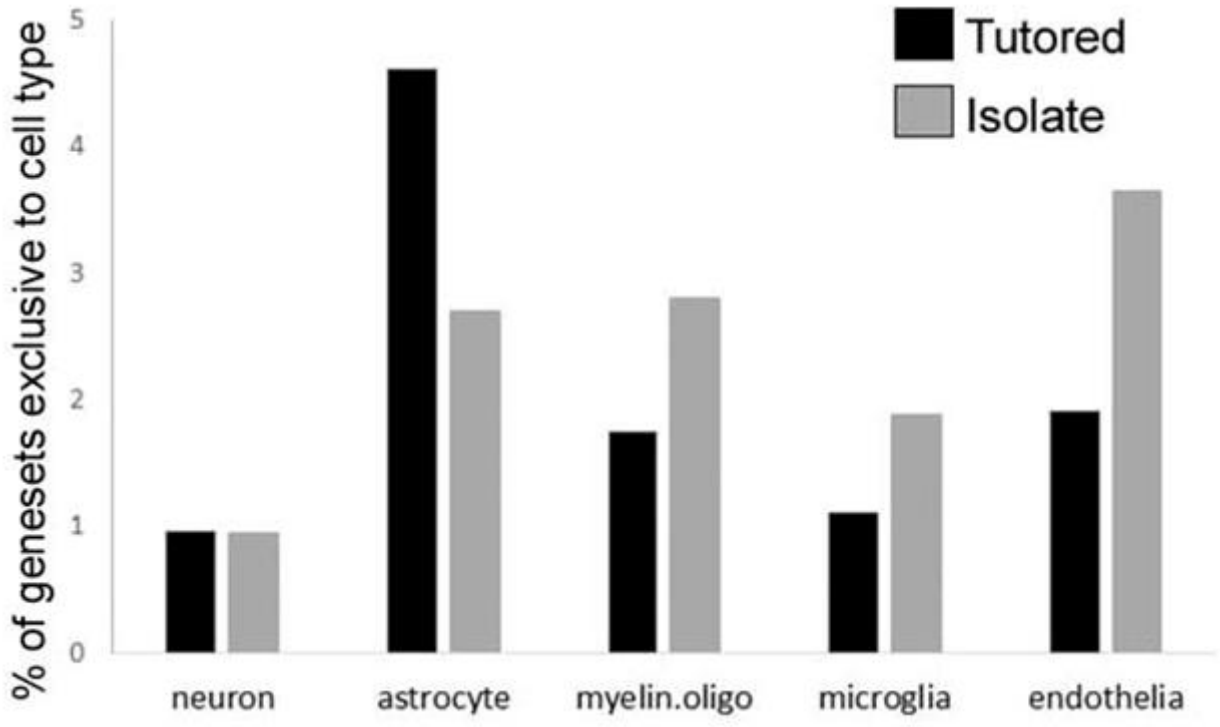

SUPPLEMENTAL EXPERIMENTAL PROCEDURES

Procedures were in accordance with the National Institute of Health guidelines for the care and use of animals for experimental procedures and approved by the University of Chicago Institutional Animal Care and Use Committee (ACUP #72220).

P67 song analysis

We recorded the birds with webcams placed unobtrusively within the housing chambers starting when the experimental birds were P65. We then played back these files in dedicated sound recording chambers, capturing song with Sound Analysis 2011 [1]. Sound files from the Tutored condition were manually sorted for the adult male tutor song and the Tutored male that lived with him. Isolate song bouts were also identified. Songs produced by birds P65-67 are still imprecisely structured but we could identify repeated syllable motifs for all experimental birds. One bout from each tutor was used for Asymmetric mean-value analysis and compared to 10 bouts each of the appropriate Tutored bird's song and each of the Isolate birds' songs. This analysis considers the adult tutor song as a template and quantifies how similar the juvenile's song is to it. We acquired song similarity scores for the Tutored birds by comparing 10 bouts of their recorded song to the song of the specific adult tutor male they lived with P30-67. We also compared 10 bouts of song produced by each Isolate bird with all of the adult tutor males used in each replicate of the experiment. By definition, there is no possible way that the Isolate songs can be copies of any of the adult tutors, so their similarity scores provide a measure of how similar a song can be to any one of the tutors based simply on conspecific acoustic patterning, given no possibility of learning. The expectation is that if Tutored birds were learning from their tutors, their song similarity scores would be significantly higher than any of the Isolate bird's were when compared to their tutor. The highest song similarity score was used for each Isolate bird in statistical testing. T-tests using song similarity scores at $\alpha < 0.05$ were used to test that the Tutored songs were more similar to

the tutor's song than the Isolates', indicating distinct levels of song learning and therefore the association with a closed or open CP at P67.

ChIPseq

The auditory forebrain is required for tutor song memorization [2-4]. The auditory forebrain is a discrete brain region visible with the naked eye and easily dissected [5-7]. It is neuroanatomically separable from, and projects to, areas within the motor circuitry including HVC and RA [7-9]. The auditory forebrain includes three major intricately interconnected subregions – field L (primary auditory cortex), and caudomedial nidopallium (NCM) and caudomedial mesopallium (CMM) which are functionally analogous to secondary auditory cortex - and heterogeneous cell types [7, 9]. Experiments that disrupt molecular signaling in as little as 15% of the secondary auditory forebrain prevent normal levels of tutor song copying in juvenile males [2, 3]. Thus, for this pioneering experiment, we assessed the chromatin profile in the entire area, as a functional unit.

For P67 Isolate and Tutored sample ChIPseq, we used 10µg chromatin with 5µl of antibody (Active Motif, #39161) for H3K9me3; 10µg chromatin with 4µg of antibody (Millipore, #07-449) for H3K27me3; 7µg chromatin with 3µl of antibody (Active Motif, #39159) for H3K4me3; and 10µg chromatin with 4 µg of antibody (Abcam, #ab5095) for RNA Pol2. Prior to ChIP, antibodies were verified to bind in zebra finch brain with Western blots. Input control sequencing was performed on a sample that combined P67 Isolate and Tutored chromatin in equal proportions. To obtain sufficient chromatin to do four ChIPseq runs plus an Input control on the same sample, bilateral auditory forebrains from four individuals from each group were pooled. We also combined both auditory forebrains from four individuals for P32 ChIPseq data, and performed ChIP with the same antibodies at the same quantities as in the P67 ChIPseq, though we used 8µg of P32 chromatin. Input control was the P32 tissue pool. Reads were

obtained from NextSeq (Illumina, San Diego, CA). Chromatin isolation, ChIP, and DNA sequencing were performed at Active Motif (Carlsbad, CA).

Antibody-chromatin complexes were captured by the addition of protein G magnetic beads and the beads were washed once with IP dilution buffer, twice with wash buffer 1 (20 mM Tris-HCl pH 8, 2 mM EDTA, 1% Triton X-100, 0.1% SDS, 150 mM NaCl), once with wash buffer 2 (20 mM Tris-HCl pH 8, 2 mM EDTA, 1% Triton X-100, 0.1% SDS, 500 mM NaCl), once with wash buffer 3 (10 mM Tris-HCl pH 8, 1 mM EDTA, 250 mM LiCl, 1% NP-40, 1% deoxycholate), and once with TE (10 mM Tris-HCl pH 8, 1 mM EDTA). DNA-protein complex was eluted twice with 100 µl elution buffer (25 mM Tris-HCl pH 7.5, 10 mM EDTA, 0.5% SDS) at 65°C for 15 min with shaking at 1200 rpm (Eppendorf ThermoMixer C). Eluted chromatin was treated with 10 mg of RNase A at 37°C for 1 h followed by proteinase K at 50°C for 2 h. Samples were then de-crosslinked at 65°C for 5 h. Reverse crosslinked DNA was purified by a PCR purification column (Qiaquick PCR purification, Qiagen), and eluted with 150 µl of buffer EB (10 mM Tris-HCl pH 8) for qPCR. Small aliquots of input chromatin samples were reverse crosslinked, RNase A, proteinase K digested and purified with PCR purification columns as described above. The concentration of the purified DNA was measured with Qubit Fluorometric Quantitation (Invitrogen) as a reference for the amount of chromatin used in each ChIP reaction. ChIP and input DNA libraries were prepared for Illumina sequencing using all of the DNA from the ChIP reaction. Libraries were prepared using the standard consecutive enzymatic steps of end-polishing, dA-addition, and adaptor ligation. The adaptor-ligated libraries were amplified with barcoded primers for 15 cycles, then purified using Agencourt AMPure XP beads and quantified to assess quality of the amplification reactions.

ChIPseq analysis

Peak calling. Single end 75 bp sequences (NextSeq500, Illumina) were mapped to the zebra finch genome assembly (Ensembl genebuild taeGut3.2.4) with BWA, using default settings to align untrimmed sequences uniquely, with no more than 2 mismatches, and duplicate reads were removed [10]. Only reads passing these criteria were inputted to SICER v1.1 to call peaks [11]. We set peak island window size to 200bp; gap size was set to 600bp for H3K9me3, H3K27me3, and RNA Pol2; gap size for H3K4me3 was 200bp; default settings for other parameters such as effective genome size (0.86) were employed [11, 12]. Peaks were called at a statistical cutoff compared to Input at 10E-5. We also used SICER to perform differential analysis between Isolate and Tutored samples for all four ChIPseq datasets with the same peak call parameters. Peaks were assigned to genes if they were within 10kb of NCBI gene models to capture genes adjacent to H3K9me3 and H3K27me3 peaks, which are typically found in intergenic regions (see Figure 1). For downstream differential gene-level analysis, we used the datasets of exclusive differential peaks with statistical threshold set at 10E-5, to allow for complexity of brain tissue composed of multiple cell types; we found <3% overlap of peaks between Isolate and Tutored datasets within a PTM or Pol2 run at this threshold, indicating specificity. NCBI genes were annotated for Ensembl gene and transcript identifiers, and Hugo Gene Nomenclature Consortium names (HGNC) with Biomart [13].

Bioinformatic analysis of gene sets. For GO and KEGG analysis, we converted Entrez gene IDs to Ensembl gene IDs to assay for significantly over- and under-represented categories or pathways. We used a custom algorithms for the zebra finch genome (http://www.ark-genomics.org/tools/GOfinch, www.ark-genomics.org/tools/KEGGfinch;[14] with the Ensembl gene set v84 as the universe. GO output includes annotation for Molecular Function, Biological Process, and Cellular component hierarchies. To ask what protein classes and biological pathways were represented in the datasets, we entered HGNC

gene identifiers into geneontology.org and obtained Panther Protein Classes. We tested if there were particular transcription factors predicted to bind to an overrepresented subset of the marked genes. We used a custom algorithm for Position Weight Matrices (PWM) built for analysis against the zebra finch assembly (taeGut3.2.4), using our datasets against the Ensembl transcript v84 universe [15]. We analyzed 5kb upstream/2kb downstream of predicted transcriptional start site (TSS), and, because the 5' ends of gene models are often truncated in the Ensembl models, 20kb upstream of the TSS and then combined outputs to generate a single list of uniquely overrepresented PWM for Isolate and Tutored genesets. The PWM analytical tool became inaccessible before Replicate 2 data were collected, thus we could not acquire a comparable output. As a prediction of how the PTMs and Pol2 transcription might be distributed across different cell types present in auditory forebrain, we used a database created from cell type-specific cultures to find which of our differential genes were among the top 100 genes that distinguish major cell types (neurons, astrocytes, microglia, myelinating oligodendrocytes, and endothelial cells; http://web.stanford.edu/group/barres_lab/brain_rnaseq.html;[16]. To test for statistical differences between the Tutored and Isolate gene set populations, we calculated the Z-score for two population proportions, with $\alpha < 0.05$.

RNAseq

For RNAseq analysis, we raised an independent set of Tutored and Isolate P67 males under the same conditions as the ChIPseq experiment. Eight auditory forebrain samples, each representing a single animal, were sequenced for each of the two groups. Total RNA libraries were constructed with Illumina oligo-dT primed TruSeq v2 RNA kits (Illumina) to generate 50nt single-end reads off an Illumina HiSeq2000. Raw read quality was assessed with FastQC (www.bioinformatics.babraham.ac.uk/projects/fastqc/), which showed scores above 32. Reads were trimmed with TrimGalore (www.bioinformatics.babraham.ac.uk/projects/trim_galore/) and aligned to

the genome assembly (taeGut3.2.4) with TopHat 2.1 using default settings for nucleotide mismatches, gap distances, and intron size [17]. We ran HTSeq 0.6.1 (strandedness set for "no"; https://htseq.readthedocs.io) to count the number of reads aligned to gene models, then DESeq2 (v 1.18.1) to identify transcripts represented differentially in the Isolate compared to Tutored samples (α < 0.05;[18, 19].

Immunohistochemistry and *in situ* hybridization

Brains. We raised another set of P67 males under Tutored and Isolate conditions (n=5 Tutored, n=7 Isolate). At P67, birds were transcardially perfused, first with 0.1M phosphate-buffered saline (PBS) and then with 4% paraformaldehyde (PFA) in 0.025M PBS. Whole brains were dissected and post-fixed overnight in 4% PFA at 4°C. Brains were gelatin-embedded (8% gelatin in 0.1M PBS), and incubated overnight in PFA. Gelatin-embedded brains were cryoptotected by successive incubations in 15% and 30% sucrose in 0.1M PBS. A cryostat was used to section brains (20µm) in a series for molecular analysis of all genes/proteins across the ~1mm lateral extent of the auditory forebrain. Two series were thaw-mounted onto Superfrost Plus slides (Thermo Fisher; Waltham, MA USA) and stored at -80°C for *in situ* hybridization; the others were collected as free-floating sections in 0.1M PBS and stored at 4°C for immunohistochemistry.

Molecular biology. To label oligodendrocytes, we hybridized one series of thaw-mounted sections with a Digoxigenin (DIG)-labeled myelin proteolipid protein (PLP) antisense riboprobe. Riboprobes were *in vitro* transcribed from linearized *T.guttata* EST FE722130, and purified before use (RNeasy, Qiagen; Hilden, Germany). Slides with thaw-mounted sections were removed from -80°C, and processed for in situ hybridization as described previously [6, 20].

To label mature neurons, astrocytes, and endothelial cells we performed immunohistochemistry for NeuN, glutamine synthetase (GluL), and zona occludens-1 (ZO1), respectively. The primary antibodies used were: mouse anti-NeuN (EMD Millipore #MAB377; Burlington, MA, USA), mouse anti-GLUL (Atlas Antibodies # AMAb91103; Bromma, Sweden), and mouse anti-ZO-1 (Thermo Fisher #ZO1-1A12). Sections were permeabilized with 0.1 M PBS containing 0.03% Triton-X. After three, 10 minute washes with 0.1 M PBS containing 0.5% Tween-20 (PBST), endogenous peroxidases were exhausted with 2% H_2O_2 in PBST. Sections were again washed (3x, for 10 minutes each) and blocked for 30 minutes at room temperature in 3% normal horse serum (NHS; Vector Laboratories, Cat# S-2000; Burlingame, CA, USA). Sections were incubated in primary antibody prepared in PBST containing 1% normal serum either overnight (NeuN, GluL) or for 48 hours (ZO1). Sections were washed 3x 10 minutes in PBST. For NeuN and GluL, sections were incubated for 2 hours at room temperature in biotinylated secondary antibodies prepared in PBST containing 1% normal serum (1:100; Vector Laboratories, Cat# BA-2000). After washing with PBST (3x, 10 minutes each), sections were incubated with avidin-biotin complex (ABC, Vector Laboratories, Cat# PK6100) for 30 minutes at room temperature. Following 0.1M PBS washes (3x, 10 minutes each), the peroxidase complex was visualized with DAB (Sigma-Aldrich USA) containing 0.003% H_2O_2 in 0.1M PBS. Sections were mounted, dehydrated, cleared, and coverslipped with Permount (Thermo Fisher). For ZO1, sections were incubated for 2 hours in Dylight 488 Horse anti-mouse IgG secondary (1:100; Vector Laboratories Cat# DI2649) prepared in PBST containing 1% normal serum and DAPI at room temperature. Sections were then washed (3x 10 minutes in 0.1M PBS) mounted on Superfrost Plus slides (Thermo Fisher), dried overnight in the dark, and coverslipped with 2.5% PVA containing 0.5% DABCO.

Image acquisition and analysis. For NeuN, PLP, and ZO-1, images were captured using the 4X objective on an Olympus IX81 microscope (Olympus Corporation of the Americas, Center Valley, PA) with a

Hamamatsu Orca Flash 4.0 sCMOS camera (Hamamatsu Photonics, Skokie, IL) running Slidebook 5.0 software (Intelligent Imaging Innovations). For GluL, images were constructed from 40X digital image files created with a 3D Histech Pannoramic Scan whole slide scanner and software (Perkin Elmer, Waltham, MA) equipped with a Stingray F146C color camera (Allied Vision Technologies, Stadtroda, Germany).

Both cell density analysis (NeuN, PLP, and GluL) and measurements of the percent area stained (ZO1) were conducted using FIJI [21]. For cell density analysis, we obtained cell count numbers from intensity-thresholded images using the Analyze Particles command. Cell counts were divided by the area of the Region of Interest (ROI) selected (here, the boundaries of the auditory forebrain, which are visible in light microscopy images) to calculate a cell density measure. Because endothelial cells are grouped tightly together, we assessed the %Area that the ZO1 staining occupied, rather than a normalized cell count measure, in the ROI using the FIJI Measurement tool, after thresholding image intensities. Measures were averaged across all sections for each bird to obtain an individual bird mean. T-tests with $\alpha < 0.05$ were used to assess statistically significant differences between Tutored and Isolate measures for each cell type.

SUPPLEMENTAL REFERENCES

1. Tchernichovski O., Nottebohm F., Ho C.E., Pesaran B., Mitra P.P. 2000 A procedure for an automated measurement of song similarity. *Anim Behav* **59**(6), 1167-1176. (doi:10.1006/anbe.1999.1416).
2. Ahmadiantehrani S., London S.E. 2017 Bidirectional manipulation of mTOR signaling disrupts socially mediated vocal learning in juvenile songbirds. *Proceedings of the National Academy of Sciences* **114**(35), 9463-9468. (doi:10.1073/pnas.1701829114).
3. London S.E., Clayton D.F. 2008 Functional identification of sensory mechanisms required for developmental song learning. *Nat Neurosci* **11**(5), 579-586. (doi:10.1038/nn.2103).
4. Yanagihara S., Yazaki-Sugiyama Y. 2016 Auditory experience-dependent cortical circuit shaping for memory formation in bird song learning. *Nature Communications* **7**, 11946. (doi:10.1038/ncomms11946 http://www.nature.com/articles/ncomms11946#supplementary-information).

5. Cheng H.Y., Clayton D.F. 2004 Activation and habituation of extracellular signal-regulated kinase phosphorylation in zebra finch auditory forebrain during song presentation. *J Neurosci* **24**(34), 7503-7513. (doi:10.1523/JNEUROSCI.1405-04.2004).
6. London S.E., Dong S., Replogle K., Clayton D.F. 2009 Developmental shifts in gene expression in the auditory forebrain during the sensitive period for song learning. *Dev Neurobiol* **69**(7), 437-450.
7. Vates G.E., Broome B.M., Mello C.V., Nottebohm F. 1996 Auditory pathways of caudal telencephalon and their relation to the song system of adult male zebra finches. *The Journal of comparative neurology* **366**(4), 613-642. (doi:10.1002/(SICI)1096-9861(19960318)366:4<613::AID-CNE5>3.0.CO;2-7).
8. Bauer E.E., Coleman M.J., Roberts T.F., Roy A., Prather J.F., Mooney R. 2008 A synaptic basis for auditory-vocal integration in the songbird. *J Neurosci* **28**(6), 1509-1522. (doi:10.1523/jneurosci.3838-07.2008).
9. Theunissen F.E., Amin N., Shaevitz S.S., Woolley S.M.N., Fremouw T., Hauber M.E. 2004 Song Selectivity in the Song System and in the Auditory Forebrain. *Annals of the New York Academy of Sciences* **1016**(1), 222-245. (doi:10.1196/annals.1298.023).
10. Li H., Durbin R. 2009 Fast and accurate short read alignment with Burrows-Wheeler transform. *Bioinformatics (Oxford, England)* **25**(14), 1754-1760. (doi:10.1093/bioinformatics/btp324).
11. Xu S., Grullon S., Ge K., Peng W. 2014 Spatial Clustering for Identification of ChIP-Enriched Regions (SICER) to Map Regions of Histone Methylation Patterns in Embryonic Stem Cells. *Methods in molecular biology (Clifton, NJ)* **1150**, 97-111. (doi:10.1007/978-1-4939-0512-6_5).
12. Pepke S., Wold B., Mortazavi A. 2009 Computation for ChIP-seq and RNA-seq studies. *Nat Meth* **6**(11s), S22-S32.
13. Yates A., Akanni W., Amode M.R., Barrell D., Billis K., Carvalho-Silva D., Cummins C., Clapham P., Fitzgerald S., Gil L., et al. 2015 Ensembl 2016. *Nucleic Acids Research*. (doi:10.1093/nar/gkv1157).
14. Wu X., Watson M. 2009 CORNA: testing gene lists for regulation by microRNAs. *Bioinformatics (Oxford, England)* **25**(6), 832-833. (doi:10.1093/bioinformatics/btp059).
15. Blatti C., Sinha S. 2014 Motif enrichment tool. *Nucleic Acids Res* **42**(Web Server issue), W20-25. (doi:10.1093/nar/gku456).
16. Zhang Y., Chen K., Sloan S.A., Bennett M.L., Scholze A.R., O'Keeffe S., Phatnani H.P., Guarnieri P., Caneda C., Ruderisch N., et al. 2014 An RNA-Sequencing Transcriptome and Splicing Database of Glia, Neurons, and Vascular Cells of the Cerebral Cortex. *The Journal of Neuroscience* **34**(36), 11929-11947. (doi:10.1523/jneurosci.1860-14.2014).
17. Kim D., Pertea G., Trapnell C., Pimentel H., Kelley R., Salzberg S.L. 2013 TopHat2: Accurate alignment of transcriptomes in the presence of insertions, deletions and gene fusions. *Genome biology* **14**(4). (doi:10.1186/gb-2013-14-4-r36).
18. Anders S., Pyl P.T., Huber W. 2015 HTSeq—a Python framework to work with high-throughput sequencing data. *Bioinformatics (Oxford, England)* **31**(2), 166-169. (doi:10.1093/bioinformatics/btu638).
19. Love M.I., Huber W., Anders S. 2014 Moderated estimation of fold change and dispersion for RNA-seq data with DESeq2. *Genome biology* **15**(12), 550. (doi:10.1186/s13059-014-0550-8).
20. Jin H., Clayton D.F. 1997 Localized changes in immediate-early gene regulation during sensory and motor learning in zebra finches. *Neuron* **19**(5), 1049-1059.
21. Schindelin J., Arganda-Carreras I., Frise E., Kaynig V., Longair M., Pietzsch T., Preibisch S., Rueden C., Saalfeld S., Schmid B., et al. 2012 Fiji: an open-source platform for biological-image analysis. *Nat Methods* **9**(7), 676-682. (doi:10.1038/nmeth.2019).